IEEE Access
Multidisciplinary | Rapid Review | Open Access Journal

Received October 12, 2018, accepted October 27, 2018, date of publication November 23, 2018, date of current version January 4, 2019.

Digital Object Identifier 10.1109/ACCESS.2018.2882710

Hammerstein Adaptive Impedance Controller for Bionic Wrist Joint Actuated by Pneumatic Muscles

HUI YANG, (Student Member, IEEE), XIFENG GAO, (Student Member, IEEE), YANG CHEN, (Student Member, IEEE), AND LINA HAO, (Member, IEEE)
School of Mechanical Engineering and Automation, Northeastern University, Shenyang 110819, China

Corresponding author: Lina Hao (haolina@me.neu.edu.cn)

This work was supported in part by the National High Technology Research and Development Program of China (863 Program) under Grant 2015AA042302 and in part by the National Natural Science Foundation of China under Grant 61573093 and Grant U1613205.

ABSTRACT For the nonlinear, time-variable and unpredictable environment (such as the manipulator workspace that has many random and moveable obstacles), a Hammerstein adaptive (HA) impedance controller based on a Hammerstein impedance model is proposed in this paper. The model consists of a static nonlinear element and a linear dynamic element, which can describe the nonlinearity of the environment. Then, an adaptive law is designed by a Lyapunov function, which can adjust the parameters of the static nonlinear element, so that the model has good adaptability and robustness for the environment. By introducing a parameters self-adjust model-free adaptive controller as the inner position controller, the HA impedance control system is built, which does not require the knowledge of the robot dynamics. In order to verify the force-control performance of the proposed control scheme, some simulations and experiments are done on a bionic wrist joint actuated by pneumatic muscles. Compared with the conventional impedance controller with constant parameters, experimental results demonstrate that HA impedance controller has better force tracking characteristic and can restrict the contact force effectively, no matter how the external environment changes, which increases the safety between robots and humans or operation objects.

INDEX TERMS Hammerstein impedance model, adaptive law, PSA-MFAC, force control, bionic wrist joint.

I. INTRODUCTION

In recent years, robots have more opportunities to work for humans in daily life, which increases the chances of physical interactions between robots and humans, other robots or various daily necessities. Hence, the adoption of compliance control algorithms is necessary to ensure the safety of humans and breakage prevention of robots and operation objects. At present, compliance control algorithms mainly contain the impedance control and the hybrid force/position control. Impedance control algorithm is originally proposed by Hogan [1] in 1985. The method is to keep an impedance relationship between the manipulator position error and the contact force with environment, instead of tracking a desired motion or force. Compared with hybrid force/positon control, impedance control considers dynamic characteristics of a manipulator and doesn't need specific mission arrangements, which makes it widely adopted in manipulator compliance control [2], [3]. In the face of the time-variable and unpredictable external environment, impedance control with constant impedance gains cannot obtain a good performance [4], [5]. Therefore, many work on adaptive impedance control has been done in past several years. Ficuciello proposed a variable impedance controller for 7-degree-of-freedom manipulator. The controller with a suitable modulation strategy has better performance than the constant impedance, and allows reaching a favorable compromise between accuracy and execution time [6]. Khoshdel presented a variable impedance control based on the voltage control strategy for a lower-limb rehabilitation robot. The impedance parameters of the controller were evaluated by Interval Type-2 Fuzzy Logic (IT2F1), which makes the controller have good performance in therapeutic exercises [7]. Ryuta proposed an adaptive impedance control law for a variable stiffness actuator (VSA). By using the relationship between motion and passive impedance, the control law adaptively adjusts the passive stiffness to minimize the energy consumption, which doesn't

need explicit desired impedance [8]. Koivumäki proposed a novel non-switching impedance control scheme for hydraulic robotics manipulators. The dynamic relationship between the manipulator and the environment was analyzed by using a virtual power flow, and then the impedance behavior was designed for the system [9]. The above methods have good robustness and environment adaptability, which ensures the robotic systems have good safety and compliance. But these control schemes with inner force controller always need accuracy dynamic models of robotic systems which are difficult to be obtained in practice [10]–[14].

In order to achieve impedance control with less or no the knowledge of robotics dynamics, the impedance control schemes with a learning controller or a model-free position controller are presented [15]–[17]. He W developed an impedance control scheme with an adaptive neural network (NN) controller for an n-link robotic manipulator. From the simulation results, the control algorithm has a good impedance tracking performance [18]. Kim *et al.* [19] proposed a position-based impedance controller for force tracking of the wall-cleaning unit, and the controller doesn't use the dynamic model of the control object and has a good force tracking performance. But all the above methods are based on the conventional linear impedance model which cannot well describe the nonlinearity of the external environment.

Hammerstein model is a kind of typical nonlinear models, and can describe many nonlinear problems, such as biological systems, electric systems, smart material systems, chemical process systems and so on [20]–[24]. In this paper, we design Hammerstein impedance model for depicting the nonlinearity of the external environment. The static nonlinear element of the model is a third order nonlinear polynomial, and the conventional impedance model is selected as the linear dynamic element of the model. For improving the adaptability and robustness of the model, an adaptive law is designed via a Lyapunov function. By introducing a parameters self-adjust model-free adaptive controller (PSA-MFAC), the Hammerstein adaptive (HA) impedance control scheme without the knowledge of robotic dynamics is proposed. In order to verify the force control performance of the proposed control scheme, some simulations and experiments are conducted by choosing a pneumatic muscle actuated bionic wrist joint as the control object, which demonstrate the effectiveness of HA impedance control scheme.

This paper is organized as follows. Section 2 introduces the conventional impedance controller. Section 3 presents Hammerstein impedance model and designs an adaptive law to adjust the parameters of the model. Section 4 verifies the force control tracking characteristic and the environmental adaptability by simulations. Section 5 gives the experimental set up and results to further verify the control performance of the proposed controller. Section 6 summarizes the main contribution of this paper.

II. CONVENTIONAL IMPEDANCE CONTRAL

A manipulator end effector will be constrained as soon as it contacts with the external environment. The relationship between the end effector position and the contact force is a dynamic system and can be expressed as

$$\mathbf{F} = M_e\Delta\ddot{\mathbf{x}} + C_e\Delta\dot{\mathbf{x}} + K_e\Delta\mathbf{x} \tag{1}$$

where $\mathbf{F} \in \mathbf{R}^{3\times1}$ is the contact force between the end effector and the environment, K_e is the environment stiffness coefficient, C_e is the environment damping coefficient, M_e is the environment inertia coefficient, and $\Delta\mathbf{x} = \mathbf{x} - \mathbf{x}_e \in \mathbf{R}^{3\times1}$ is the displacement vector of the end effector after contacting with the environment, $\mathbf{x} \in \mathbf{R}^{3\times1}$ is the position of the end effector, $\mathbf{x}_e \in \mathbf{R}^{3\times1}$ is the positon of the external environment. If the manipulator moves in a very low speed, the effects of inertia and damping can be neglected, and then (1) can be treated as the linear system which is represented as

$$\mathbf{F} = K_e(\mathbf{x} - \mathbf{x}_e) \tag{2}$$

From literature [1], the conventional desired impedance model is described as

$$\begin{aligned}\mathbf{F} - \mathbf{F}_r &= M_d(\ddot{\mathbf{x}} - \ddot{\mathbf{x}}_e) + C_d(\dot{\mathbf{x}} - \dot{\mathbf{x}}_e) + K_d(\mathbf{x} - \mathbf{x}_e) \\ &\quad - (M_d(\ddot{\mathbf{x}}_r - \ddot{\mathbf{x}}_e) + C_d(\dot{\mathbf{x}}_r - \dot{\mathbf{x}}_e) + K_d(\mathbf{x}_r - \mathbf{x}_e)) \\ &= M_d(\ddot{\mathbf{x}} - \ddot{\mathbf{x}}_r) + C_d(\dot{\mathbf{x}} - \dot{\mathbf{x}}_r) + K_d(\mathbf{x} - \mathbf{x}_r)\end{aligned} \tag{3}$$

where M_d is the desired inertia coefficient, C_d is the desired damping coefficient, K_d is the desired stiffness coefficient, $\mathbf{F}_r \in \mathbf{R}^{3\times1}$ is the desired contact force, and $\mathbf{x}_r \in \mathbf{R}^{3\times1}$ is the desired position. By adjustment, M_d, C_d and K_d should be approximately equaled to M_e, C_e and K_e, respectively.

Set $\Delta\mathbf{x}' = \mathbf{x} - \mathbf{x}_r$ and $\mathbf{F}_e = \mathbf{F} - \mathbf{F}_r$, (3) can be written as

$$\mathbf{F}_e = M_d\Delta\ddot{\mathbf{x}}' + C_d\Delta\dot{\mathbf{x}}' + K_d\Delta\mathbf{x}' \tag{4}$$

According to (4), the transfer function of impedance control is expressed as

$$G_F(s) = \frac{\mathbf{F}_e(s)}{\Delta\mathbf{x}'(s)} = M_d s^2 + C_d s + K_d \tag{5}$$

From (5), the end effector position correction $\Delta\mathbf{x}'$ can be obtained that

$$\Delta\mathbf{x}'(s) = \frac{\mathbf{F}_e(s)}{M_d s^2 + C_d s + K_d} \tag{6}$$

and then the desired position $\mathbf{x}_r$ is expressed as follows

$$\begin{cases}\mathbf{x}_r = \mathbf{x} - \Delta\mathbf{x}' & (\mathbf{F} \neq 0) \\ \mathbf{x}_r = \mathbf{x}_p & (\mathbf{F} = 0)\end{cases} \tag{7}$$

where $\mathbf{x}_p \in \mathbf{R}^{3\times1}$ is the planning trajectory of the end effector and the contact force $\mathbf{F}$ can be measured via a force/torque sensor. By taking $\mathbf{x}_r$ into the inner position controller, the desired impedance characteristic of the manipulator can be implemented.

III. HARDWARE EQUIPMENT

As (3) shows, the conventional impedance model is a linear model, and its impedance parameters always are set as constant. Hence, its accuracy depends on knowledge of the environment [25]. Nevertheless, the external environment has time-variation, unpredictability and nonlinearity, so the conventional impedance controller cannot track the desired contact force accurately and has a weak robustness with the changing of the environment. In this section, we propose a Hammerstein impedance model for describing the environmental nonlinearity, and design an adaptive law to increase the environmental adaptability and robustness of the model.

A. HAMMERSTEIN IMPEDANCE MODEL

Hammerstein model was first proposed by Hammerstein in 1930. The model consists of a static nonlinear element SN(·) followed by a linear dynamic element LD(z) [25], as shown in Fig. 1.

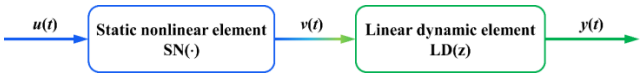

FIGURE 1. The schematic of Hammerstein model.

In Fig. 1, $u(t)$ is the input variable, $v(t)$ is the unmeasurable intermediate variable and $y(t)$ is the output variable. Each element in the model has the selectivity and diversity, so the model can describe a variety of higher-order nonlinear systems well [27], such as biological systems, artificial muscle actuators, electric systems and so on.

Because of the nonlinearity of the external environment, Hammerstein model can be used for modeling the contact environment. Then, the conventional desired impedance model is used as the linear dynamic element, and a third order nonlinear polynomial which is always used to express nonlinearity is introduced as the static nonlinear element [28], [29]. Therefore, Hammerstein desired impedance model can be represented as

$$\begin{cases} \mathbf{V}_e = \sum_{i=1}^{4} \alpha_i \mathbf{F}_e^{i-1} \\ \mathbf{V}_e = (M_d' \Delta\ddot{\mathbf{x}}' + C_d' \Delta\dot{\mathbf{x}}' + K_d' \Delta\mathbf{x}') \end{cases} \tag{8}$$

where $\mathbf{V}_e \in \mathbf{R}^{3\times 1}$ is the output of the static nonlinear element, the element parameters $\alpha_i > 0 (i = 1, 2, 3, 4)$, and K_{d}', C_{d}' and M_{d}' are positive impedance parameters of the linear dynamic element. If $\alpha_2 = 1$ and $\alpha_1 = \alpha_3 = \alpha_4 = 0$, (8) is the conventional impedance model. By the Laplace transform for the linear dynamic element, (8) is rewritten as

$$\begin{cases} \mathbf{V}_e = \sum_{i=1}^{4} \alpha_i \mathbf{F}_e^{i-1} \\ \Delta\mathbf{x}'(s) = \dfrac{\mathbf{V}_e}{(M_d' s^2 + C_d' s + K_d')} \end{cases} \tag{9}$$

From (7) and (9), the desired position $\mathbf{x}_r$ can be obtained.

B. ADAPTIVE LAW

Transform (9) into the state equation form expressed as follow

$$\begin{cases} \dot{\mathbf{x}}_{\mathrm{st}} = \mathbf{A}\mathbf{x}_{\mathrm{st}} + \mathbf{B}\mathbf{V}_e \\ \Delta\mathbf{x}' = \mathbf{C}\mathbf{x}_{\mathrm{st}} + \mathbf{D}\mathbf{V}_e \\ \mathbf{V}_e = \sum_{i=1}^{4} \alpha_i \mathbf{F}_e^{i-1} \end{cases} \tag{10}$$

where $\mathbf{x}_{\mathrm{st}}$ is the status variable of Hammerstein impedance model, and $\mathbf{A}$, $\mathbf{B}$, $\mathbf{C}$ and $\mathbf{D}$ the state-space matrices expressed as follows:

$$\begin{aligned} \mathbf{A} &= \begin{bmatrix} -\dfrac{C_d'}{M_d'}, & -\dfrac{K_d'}{M_d'} \\ 1, & 0 \end{bmatrix}, \quad \mathbf{B} = \begin{bmatrix} 1 \\ 0 \end{bmatrix}, \\ \mathbf{C} &= \begin{bmatrix} 0 \\ 1 \\ \dfrac{}{M_d'} \end{bmatrix}^{\mathbf{T}}, \quad \mathbf{D} = \begin{bmatrix} 0 \\ 0 \end{bmatrix}, \ \mathbf{x}_{\mathrm{st}} = \begin{bmatrix} M_d' \Delta\dot{\mathbf{x}}' \\ M_d' \Delta\mathbf{x}' \end{bmatrix} \end{aligned} \tag{11}$$

By substituting the third order nonlinear polynomial into the linear state equation, (10) can be rewritten as

$$\begin{cases} \dot{\mathbf{x}}_{\mathrm{st}} = \mathbf{A}\mathbf{x}_{\mathrm{st}} + \mathbf{B}(\tilde{\mathbf{U}}_k \boldsymbol{\alpha}) \\ \Delta\mathbf{x}' = \mathbf{C}\mathbf{x}_{\mathrm{st}} \end{cases} \tag{12}$$

where $\tilde{\mathbf{U}}_k = [\mathbf{F}_e^3, \mathbf{F}_e^2, \mathbf{F}_e, 1]$ and $\alpha = [\alpha_4, \alpha_3, \alpha_2, \alpha_1]^{\mathbf{T}}$.

Consider the Lyapunov function candidate

$$V(\mathbf{x}_{\mathrm{st}}, \boldsymbol{\alpha}) = \mathbf{x}_{\mathrm{st}}^{\mathbf{T}} \mathbf{P} \mathbf{x}_{\mathrm{st}} + \boldsymbol{\alpha}^{\mathbf{T}} \boldsymbol{\Gamma}^{-1} \boldsymbol{\alpha} \tag{13}$$

where $\mathbf{P}$ and $\boldsymbol{\Gamma}$ are symmetric positive definite constant matrices. According to the Lyapunov function, existing positive definite matrix $\mathbf{Q}$ should satisfy

$$\mathbf{P}\mathbf{A} + \mathbf{A}^{\mathbf{T}}\mathbf{P} = -\mathbf{Q} \tag{14}$$

Set $\mathbf{Q} = \begin{bmatrix} 10 \\ 01 \end{bmatrix}$, the constant matrix $\mathbf{P}$ can be calculated via (14)

$$\mathbf{P} = \begin{bmatrix} \dfrac{M_d'(K_d' + M_d')}{2C_d'K_d'} & \dfrac{M_d'}{2K_d'} \\ \dfrac{M_d'}{2K_d'} & \dfrac{M_d'^2 + C_d'^2 + K_d'^2}{2C_d'K_d'} \end{bmatrix} \tag{15}$$

Time derivation of (13) is

$$\begin{aligned} &\dot{V}(\mathbf{x}_{\mathrm{st}}, \boldsymbol{\alpha}) \\ &= \frac{1}{2}\dot{\mathbf{x}}_{\mathrm{st}}^{\mathbf{T}}\mathbf{P}\mathbf{x}_{\mathrm{st}} + \frac{1}{2}\mathbf{x}_{\mathrm{st}}^{\mathbf{T}}\mathbf{P}\dot{\mathbf{x}}_{\mathrm{st}} + \frac{1}{2}\dot{\boldsymbol{\alpha}}^{\mathbf{T}}\boldsymbol{\Gamma}^{-1}\boldsymbol{\alpha} + \frac{1}{2}\boldsymbol{\alpha}^{\mathbf{T}}\boldsymbol{\Gamma}^{-1}\dot{\boldsymbol{\alpha}} \\ &= \frac{1}{2}(\mathbf{x}_{\mathrm{st}}^{\mathbf{T}}\mathbf{A}^{\mathbf{T}} + \boldsymbol{\alpha}^{\mathbf{T}}\tilde{\mathbf{U}}_{\mathbf{k}}^{\mathbf{T}}\mathbf{B}^{\mathbf{T}})\mathbf{P}\mathbf{x}_{\mathrm{st}} + \frac{1}{2}\mathbf{x}_{\mathrm{st}}^{\mathbf{T}}\mathbf{P}(\mathbf{A}\mathbf{x}_{\mathrm{st}} + \mathbf{B}\tilde{\mathbf{U}}_{\mathbf{k}}\boldsymbol{\alpha}) \\ &\quad + \frac{1}{2}\dot{\boldsymbol{\alpha}}^{\mathbf{T}}\boldsymbol{\Gamma}^{-1}\boldsymbol{\alpha} + \frac{1}{2}\boldsymbol{\alpha}^{\mathbf{T}}\boldsymbol{\Gamma}^{-1}\dot{\boldsymbol{\alpha}} \\ &= \frac{1}{2}\mathbf{x}_{\mathrm{st}}^{\mathbf{T}}(\mathbf{A}^{\mathbf{T}}\mathbf{P} + \mathbf{P}\mathbf{A})\mathbf{x}_{\mathrm{st}} + \frac{1}{2}\boldsymbol{\alpha}^{\mathbf{T}}\tilde{\mathbf{U}}_{\mathbf{k}}^{\mathbf{T}}\mathbf{B}^{\mathbf{T}}\mathbf{P}\mathbf{x}_{\mathrm{st}} \\ &\quad + \frac{1}{2}\mathbf{x}_{\mathrm{st}}^{\mathbf{T}}\mathbf{P}\mathbf{B}\tilde{\mathbf{U}}_{\mathbf{k}}\boldsymbol{\alpha} + \frac{1}{2}\dot{\boldsymbol{\alpha}}^{\mathbf{T}}\boldsymbol{\Gamma}^{-1}\boldsymbol{\alpha} + \frac{1}{2}\boldsymbol{\alpha}^{\mathbf{T}}\boldsymbol{\Gamma}^{-1}\dot{\boldsymbol{\alpha}} \\ &= -\frac{1}{2}\mathbf{x}_{\mathrm{st}}^{\mathbf{T}}\mathbf{Q}\mathbf{x}_{\mathrm{st}} + \frac{1}{2}(\boldsymbol{\alpha}^{\mathbf{T}}\tilde{\mathbf{U}}_{\mathbf{k}}^{\mathbf{T}}\mathbf{B}^{\mathbf{T}}\mathbf{P}\mathbf{x}_{\mathrm{st}} + \boldsymbol{\alpha}^{\mathbf{T}}\boldsymbol{\Gamma}^{-1}\dot{\boldsymbol{\alpha}}) \\ &\quad + \frac{1}{2}(\mathbf{x}_{\mathrm{st}}^{\mathbf{T}}\mathbf{P}\mathbf{B}\tilde{\mathbf{U}}_{\mathbf{k}}\boldsymbol{\alpha} + \dot{\boldsymbol{\alpha}}^{\mathbf{T}}\boldsymbol{\Gamma}^{-1}\boldsymbol{\alpha}) \end{aligned} \tag{16}$$

From (16), the adaptive law can be set as

$$\dot{\boldsymbol{\alpha}} = -\boldsymbol{\Gamma}\tilde{\mathbf{U}}_{\mathbf{k}}^{\mathbf{T}}\mathbf{B}^{\mathbf{T}}\mathbf{P}\mathbf{x}_{\mathrm{st}} \tag{17}$$

Substituting (17) into (16), we have

$$\dot{V} = -\frac{1}{2}\boldsymbol{x}^{\mathbf{T}}\mathbf{Q}\boldsymbol{x} \leq 0 \tag{18}$$

It can be concluded that the impedance system is stable.

Define the positive definite matrix Γ as

$$\boldsymbol{\Gamma} = \begin{bmatrix} \gamma_1 & 0 & 0 & 0 \\ 0 & \gamma_2 & 0 & 0 \\ 0 & 0 & \gamma_3 & 0 \\ 0 & 0 & 0 & \gamma_4 \end{bmatrix} \tag{19}$$

where $\gamma_1 > 0$, $\gamma_2 > 0$, $\gamma_3 > 0$ and $\gamma_4 > 0$. From (15) and (19), the discrete form of equation (13) can be expressed as follow

$$\begin{cases} \alpha_4(k) = \alpha_4(k-1) - T\gamma_1\mathbf{F}_e^3 \\ \quad \cdot(\dfrac{M_d'^2(K_d' + M_d')(\Delta\mathbf{x}'(k) - \Delta\mathbf{x}'(k-1))}{2C_d'K_d'T} + \dfrac{M_d'^2\Delta\mathbf{x}'(k)}{2K_d'}) \\ \alpha_3(k) = \alpha_3(k-1) - T\gamma_2\mathbf{F}_e^2 \\ \quad \cdot(\dfrac{M_d'^2(K_d' + M_d')(\Delta\mathbf{x}'(k) - \Delta\mathbf{x}'(k-1))}{2C_d'K_d'T} + \dfrac{M_d'^2\Delta\mathbf{x}'(k)}{2K_d'}) \\ \alpha_2(k) = \alpha_2(k-1) - T\gamma_3\mathbf{F}_e \\ \quad \cdot(\dfrac{M_d'^2(K_d' + M_d')(\Delta\mathbf{x}'(k) - \Delta\mathbf{x}'(k-1))}{2C_d'K_d'T} + \dfrac{M_d'^2\Delta\mathbf{x}'(k)}{2K_d'}) \\ \alpha_1(k) = \alpha_1(k-1) - T\gamma_4 \\ \quad \cdot(\dfrac{M_d'^2(K_d' + M_d')(\Delta\mathbf{x}'(k) - \Delta\mathbf{x}'(k-1))}{2C_d'K_d'T} + \dfrac{M_d'^2\Delta\mathbf{x}'(k)}{2K_d'}) \end{cases} \tag{20}$$

where T is sampling period. To ensure the convergence of model parameters, α should be fulfill the following criteria

$$\begin{cases} \alpha_1 \in (0,\ 1] \\ \alpha_2 > 0 \\ \alpha_3 \in (0,\ 10] \\ \alpha_4 \in (0,\ 1] \end{cases} \tag{21}$$

According to (9) and (20), Hammerstein adaptive (HA) impedance controller is acquired.

IV. SIMULATION

In this Section, the force tracking characteristic and the environment adaptability of HA impedance controller are simulated and verified. A bionic wrist joint actuated by pneumatic muscles (PM) is chosen as the control object and shown in Fig. 2. And its inverse kinematic model is expressed as follow.

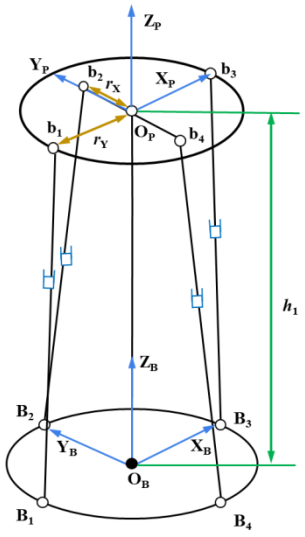

FIGURE 2. Bionic wrist joint.

$$\begin{cases} L_1 = \sqrt{4r_X^2\sin^2(\dfrac{\theta_X}{2}) + L_{01}^2 - 4rL_{01}\sin(\dfrac{\theta_X}{2})\cos(\pi - \dfrac{\theta_X}{2})} \\ L_2 = \sqrt{4r_X^2\sin^2(\dfrac{\theta_X}{2}) + L_{02}^2 - 2rL_{02}\sin(\theta_X)} \\ L_3 = \sqrt{4r_Y^2\sin^2(\dfrac{\theta_Y}{2}) + L_{03}^2 - 4rL_{03}\sin(\dfrac{\theta_Y}{2})\cos(\pi - \dfrac{\theta_Y}{2})} \\ L_4 = \sqrt{4r_Y^2\sin^2(\dfrac{\theta_Y}{2}) + L_{04}^2 - 2rL_{04}\sin(\theta_Y)} \end{cases} \tag{22}$$

where L_i ($i = 1, 2, 3,4$) is the length of the ith PM; L_{0i} is the initial length of the ith PM; r_X and r_Y are the radiuses of gyration around the X_P axis and the Y_P axis, respectively; θ_X and θ_Y are the rotation angles around the two axes, respectively.

The inner position controller is a parameters self-adjust model-free adaptive controller (PSA-MFAC) which is one of our related work. The controller doesn't need the complex dynamic model of the control object, and has good environmental adaptability and robustness. The control law [30] and the adaptive law of PSA-MFAC are represented as (23), (24) and (25).

$$\hat{\phi}_c(k) = \hat{\phi}_c(k-1) + \frac{\eta\Delta u(k-1)}{\mu + \Delta u(k-1)^2} \times (\Delta y(k) - \hat{\phi}_c(k-1)\Delta u(k-1)) \tag{23}$$

$$u(k) = u(k-1) + \frac{\rho\,\hat{\phi}_c(k)}{\lambda + \left|\hat{\phi}_c(k)\right|^2}(X_r(k+1) - y(k)) \tag{24}$$

$$\begin{cases} \eta(k+1) = \eta(k) - \left| \dfrac{(er(k) - er(k-1))}{T} \times er(k) \right| \\ \rho(k+1) = \rho(k) + \left| \dfrac{(er(k) - er(k-1))}{T} \times er(k) \right| \\ ve(k+1) = ve(k) - \left| \dfrac{(er(k) - er(k-1))}{T} \times er(k) \right| \\ \mu(k+1) = \mu(k) - ve(k) \times er(k) \\ \lambda(k+1) = \lambda(k) + ve(k+1) \times er(k) \end{cases} \tag{25}$$

where $\hat{\phi}_c(k) \in R$, $\Delta u(k) = u(k) - u(k-1)$, $\Delta y(k) = y(k) - y(k-1)$, $u(k)$ and $y(k)$ are the input and the output of the system respectively, $\lambda > 0$, $\mu > 0$, $\rho \in (0, 1]$, $\eta \in (0, 1]$, and $er(k)$ is the positon error of the system. Based on the (22) to (25), the positon control for the PM bionic wrist can be achieved.

Therefore, the HA impedance control system contains a HA impedance controller and a PSA-MFAC controller, which is described in Fig. 3.

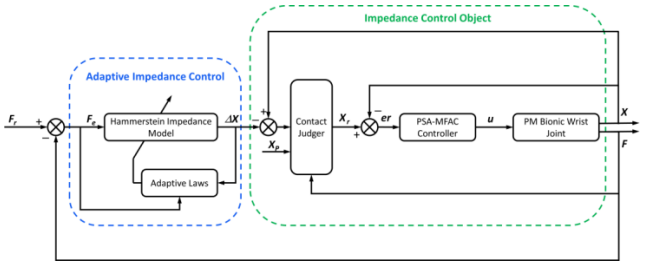

FIGURE 3. Control schematic diagram of HA impedance control system.

As Fig. 3 shows, PSA-MFAC controller, the contact judger and the bionic wrist are treated as the impedance control object, so ΔX and F are the input and the output of the system respectively.

A. SIMULATION OF FORCE TRACKING CHARACTERISTIC IN CERTAIN ENVIORNMENT CONDITONS

In this section, the force tracking characteristic of HA impedance control is simulated, and then the simulation results are compared with the conventional impedance controller. The rotation angle function of the PM bionic wrist is $\theta_Y = \pi/9\sin(\pi t/6)$, the relative initial position between the wrist joint and the end effector is (0, 0, 100), the position coordinates of the external environment are (15, 0, 98.87) and (10sin(πt/10)+20, 0, sqrt($10^2 - (10\sin(\pi t/10) + 20)^2$) respectively, the desired contact force F_r is set as 0N, 3N and 10N respectively, the impedance parameters of the environment are $K_e = 10$, $C_e = 0$, and $M_e = 0$, the parameters of the linear dynamic element are $K'_d = 1$, $C'_d = 1$, and $M'_d = 1$, the initial values of the static nonlinear element parameters are $\alpha_0 = [0, 0, 1, 0]$, the adaptive parameters are set as

$$\mathbf{\Gamma} = \begin{bmatrix} \gamma_1 & 0 & 0 & 0 \\ 0 & \gamma_2 & 0 & 0 \\ 0 & 0 & \gamma_3 & 0 \\ 0 & 0 & 0 & \gamma_4 \end{bmatrix}$$

$$= \begin{bmatrix} \dfrac{1}{K'_d + C'_d + M'_d} & 0 & 0 & 0 \\ 0 & \dfrac{1}{K'_d + C'_d} 0 & 0 & \\ 0 & 0 & \dfrac{1}{C'_d} & 0 \\ 0 & 0 & 0 & \dfrac{1}{K'_d} \end{bmatrix} \tag{26}$$

The parameters of the conventional impedance control are $K_d = 10$, $C_d = 0$, and $M_d = 0$, and the sampling period of the simulation is $T = 0.001$s. Based on the ranges of PSA-MFAC controller parameters, the initial values can be set as $\eta_0 = 1$, $\mu_0 = 1$, $\rho_0 = 0.1$, $\lambda_0 = 0.1$ and $ve_0 = 1$ respectively. Then, the simulation results about the force tracking characteristics of HA impedance controller and conventional impedance controller are shown in Figs 4 to 9.

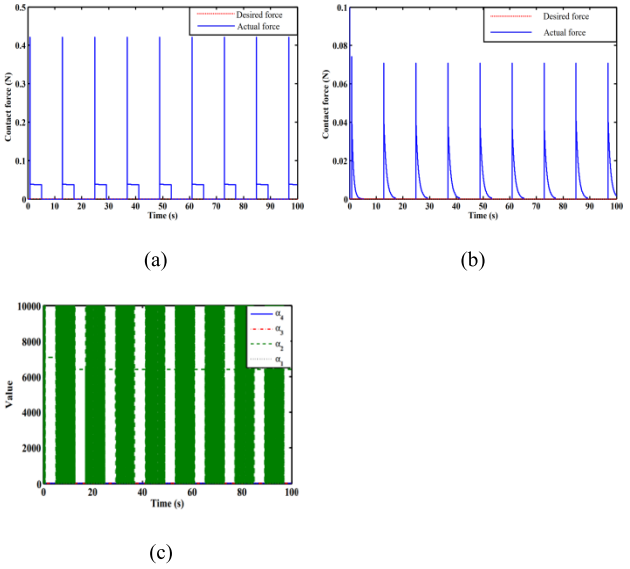

FIGURE 4. Force tracking results (F_r=0N and the external environment with unchanging position): (a) Conventional impedance controller, (b) HA impedance controller, (c) Static nonlinear element parameters of HA impedance controller.

From Figs 4(a) to 9(a), we can notice that the conventional impedance controller can effectively restrict the contact force within requirement scope, but the instantaneous value of the contact force F at the moment of impact is very high and increases with the increasing F_r. The simulation results described in Figs 4(b) to 9(b) demonstrate that HA impedance controller not only restrict the contact force obviously, but also has higher force tracking accuracy than the conventional impedance control. From Figs 4(b), 6(b) and 8(b), the tracking error is only about 0.001N when the position of external environment is unchanging. Moreover, HA impedance controller dramatically reduces the instantaneous value of F, which enhances the safety and compliance of the bionic wrist, especially when the external contact environment is moving.

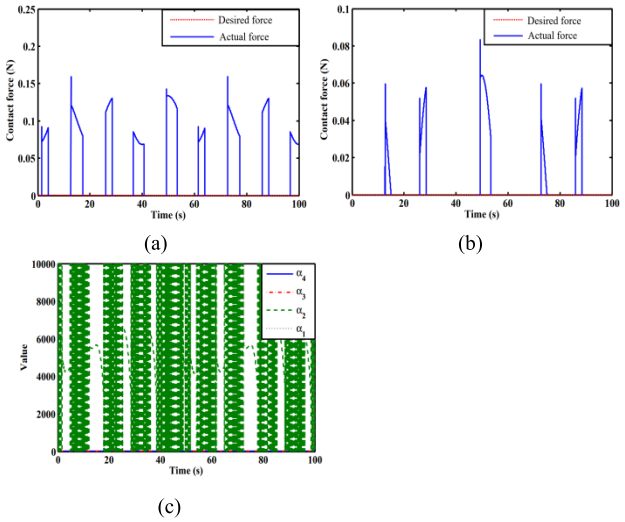

FIGURE 5. Force tracking results (F_r=0N and the external environment with time-variant position): (a) Conventional impedance controller, (b) HA impedance controller, (c) Static nonlinear element parameters of HA impedance controller.

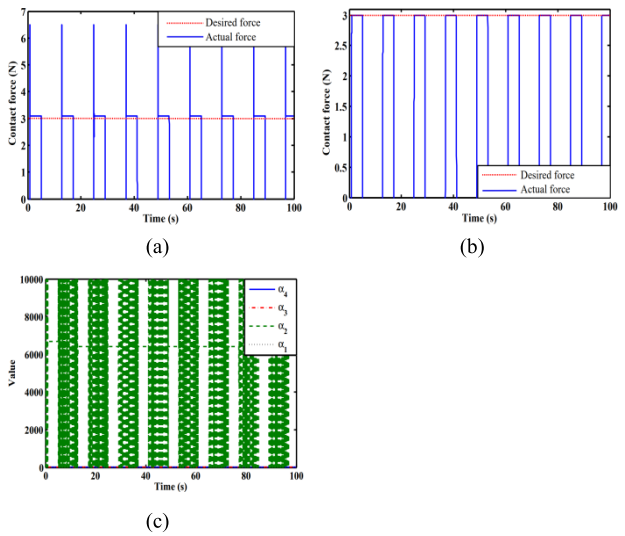

FIGURE 6. Force tracking results (Fr=3N and the external environment with unchanging position): (a) Conventional impedance controller, (b) HA impedance controller, (c) Static nonlinear element parameters of HA impedance controller.

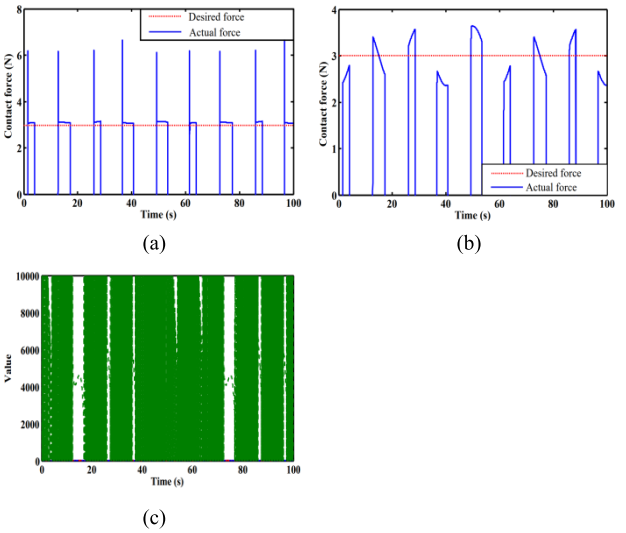

FIGURE 7. Force tracking results (F_r=3N and the external environment with time-variant position): (a) Conventional impedance controller, (b) HA impedance controller, (c) Static nonlinear element parameters of HA impedance controller.

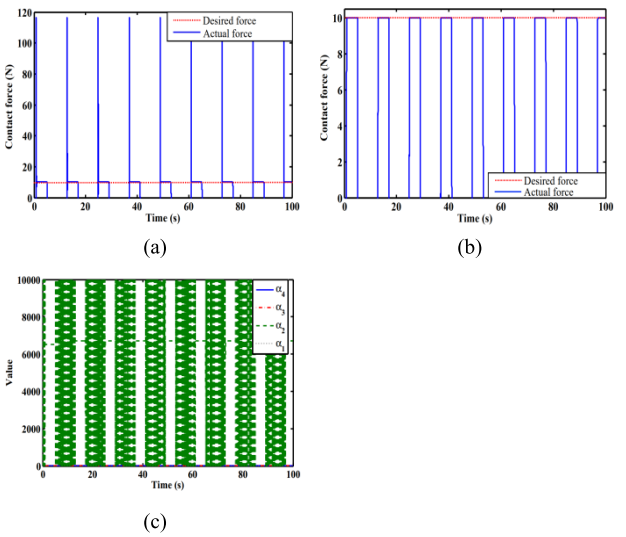

FIGURE 8. Force tracking results (F_r=3N and the external environment with time-variant position): (a) Conventional impedance controller, (b) HA impedance controller, (c) Static nonlinear element parameters of HA impedance controller.

B. SIMULATION OF FORCE TRACKING CHARACTERISTIC IN TIME-VARYING ENVIORNMENT CONDITONS

In this section, the simulation and analysis about the environmental adaptability of the proposed controller are presented. The rotation angle function of the bionic wrist is chosen as $\theta_Y = \pi/9\sin(\pi t/6)$, the relative initial position between the wrist joint and the end effector is (0, 0, 100), the desired contact force $F_r = 0$ N, and the moving trajectories of the external environment are (15, 0, 98.87) and $(X_b, 0, Z_b)$, where $X_b = 10\sin(\pi t/10)+20$ and $Z_b = \text{sqrt}(10^2 - X_b^2)$. The parameters of HA impedance controller, the conventional impedance controller and PSA-MFAC are the same as above.

The environmental model is selected as a nonlinear model expressed as follow

$$F = M_e\Delta\ddot{x} + C_e\Delta\dot{x} + K_e\Delta x^3 \tag{27}$$

where $K_e = 15\sin(\pi t/10)+15$, $C_e = 0.01$, and $M_e = 0.001$. The simulation results are reported in Figs 10 and 11.

As described in Figs 10(a) and 11(a), the conventional impedance controller with constant impedance parameters has a poor adaptability. When both the environment position and the environmental parameters are changing, the conventional impedance controller cannot effectively restrict the contact force and keep a good force tracking characteristic.

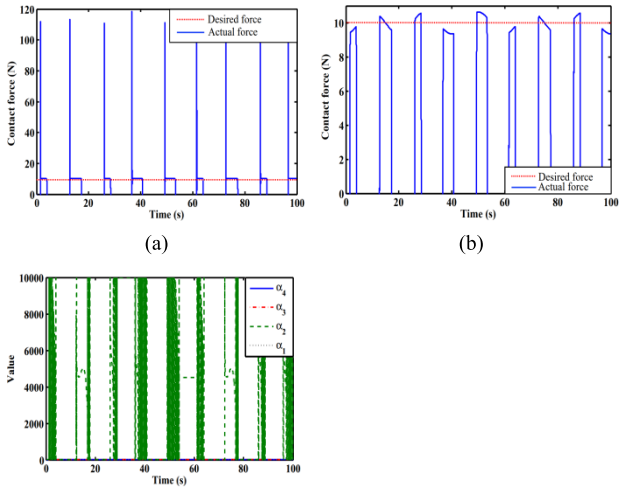

FIGURE 9. Force tracking results (F_r=10N and the external environment with time-variant position): (a) Conventional impedance controller, (b) HA impedance controller, (c) Static nonlinear element parameters of HA impedance controller.

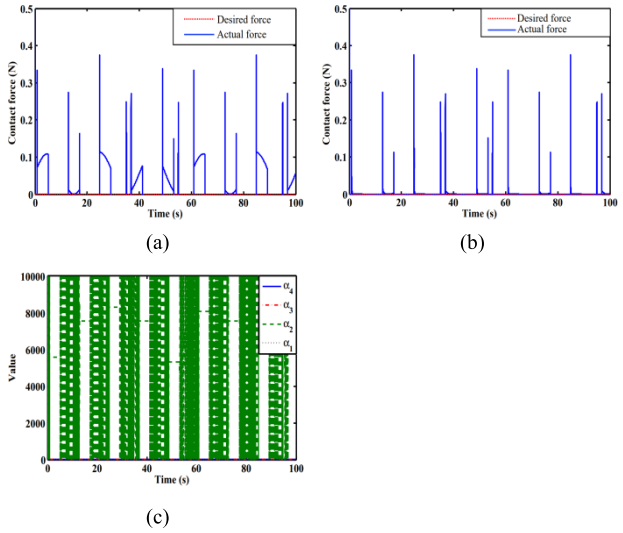

FIGURE 10. Force tracking results (the external environment with unchanging position): (a) Conventional impedance controller, (b) HA impedance controller, (c) Static nonlinear element parameters of HA impedance controller.

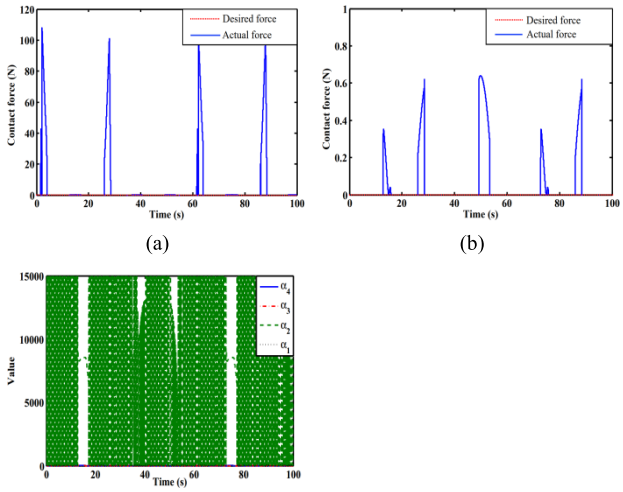

FIGURE 11. Force tracking results (the external environment with time-variant position): (a) Conventional impedance controller, (b) HA impedance controller, (c) Static nonlinear element parameters of HA impedance controller.

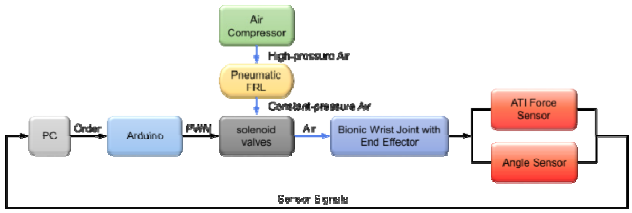

FIGURE 12. Schematic diagram of the experimental platform.

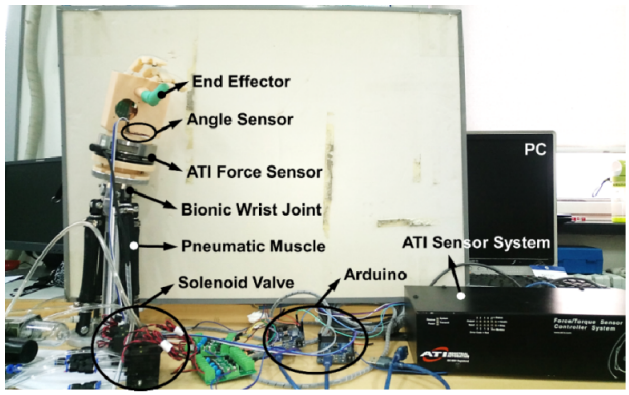

FIGURE 13. The experimental platform.

From Fig. 11(a), the value of the contact force can be more than 100N, which far exceeds the desired contact force. In contrast, HA impedance controller always has good performance in the contact force restriction and the force tracking, no matter how the external environment changes (see Figs. 10(b) and 11(b)), which illustrates that HA impedance controller has a better environmental adaptability for a nonlinear environment.

V. EXPERIMENTS

In order to further validate the proposed controller, a semi-physical experimental platform is set up, and its schematic is shown in Fig. 12. The platform consists of an air compressor as an air source, a pneumatic FRL(filter, regulator and lubricator) for keeping the air pressure to be about 4bar, 8 two-ways solenoid valves (MEAD Isonic V1, response time: 10ms), an Arduino Mega2560 board, an ATI six-axis force/torque sensor (output voltage range: ±5V, measurement range: $F_X = \pm 165$N, $F_Y = \pm 165$N,and $F_Z = \pm 495$N, measurement accuracy: 1%), an angle sensor (CJMCU-99, 13-bit resolution) and a PC with MATLAB for running the proposed control algorithm program . Moreover, 4 self-made pneumatic muscles (radius: 20mm, the maximum contraction: 21%, the working inflation pressure: 1-5bar, the

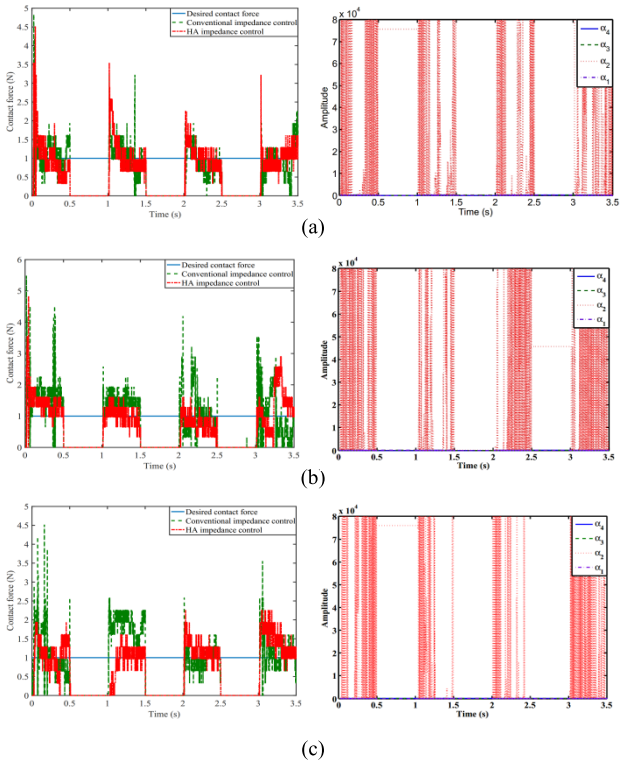

FIGURE 14. Experiment results (F_r=1N): (a) The contact object is a rubber ball, (b) The contact object is a plastic box, (c) The contact object is a tong.

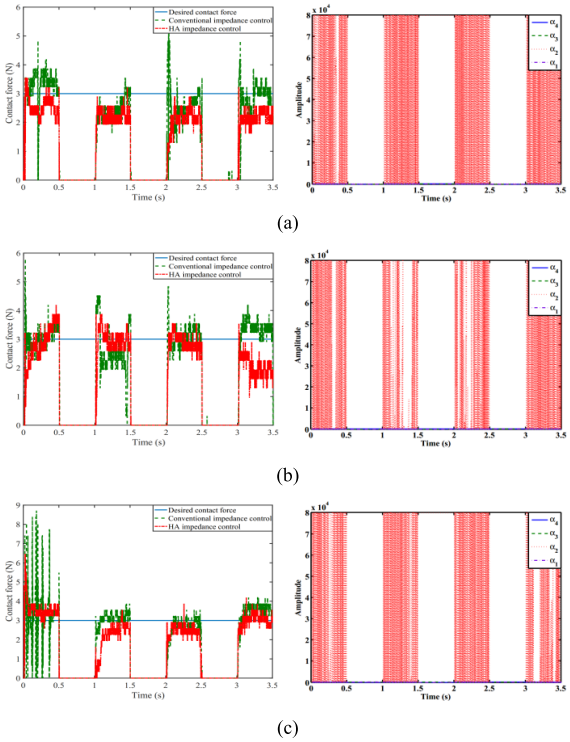

FIGURE 15. Experiment results (F_r=3N): (a) The contact object is a rubber ball, (b) The contact object is a plastic box, (c) The contact object is a tong.

maximum load: 300N) are used for actuating the bionic wrist joint. According to sensor signals and the control program, the PC sends orders to Arduino which generates PWM signals

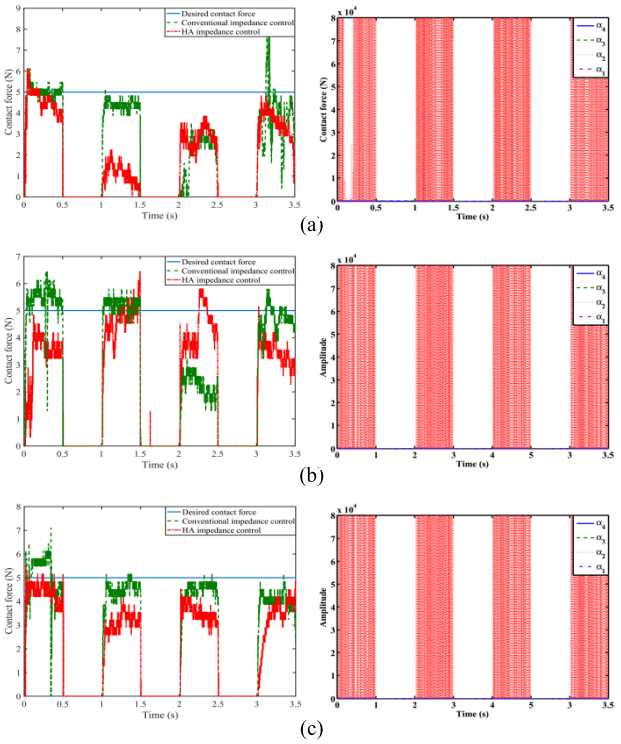

FIGURE 16. Experiment results (F_r=5N): (a) The contact object is a rubber ball, (b) The contact object is a plastic box, (c) The contact object is a tong.

to control solenoid valves, and then pneumatic muscles actuate the bionic wrist joint rotation. Based on Fig. 12, the experimental platform is built and shown in Fig. 13.

For verifying the force tracking characteristic and the environmental adaptability, the desired contact force F_r is set to 1N, 3N and 5N respectively, and we select a rubber ball, a plastic box and a tong as contact objects respectively which have different impedance parameters. The parameters of HA impedance controller and PSA-MFAC controller are the same as above. The parameters of the conventional impedance controller are $K_d = 1.5$, $C_d = 0$, and $M_d = 0$. The rotation function of the bionic wrist joint is $\theta_Y = \pi/12\text{square}(\pi t/2, 50) + \pi/12$. The experiment and comparison results are reported in Figs 14, 15 and 16.

During the experiment, the contact objects are held by a person, which doesn't keep the contact point unchanged in the contact process. Therefore, the value of contact force is sometimes changing in process of contact as shown in Fig. 16. In Figs 14 to 16, the left half parts are the comparison between the proposed controller and the conventional impedance controller on contact force tracking characteristic, and the right half parts are the adaptive parameter changing curves. From the experimental results, HA impedance controller always has good force tracking characteristic and effectively restricts the contact force within the requirement range, no matter what the contact object is. The tracking error of HA impedance controller is about ±0.5N if the contact position is unchanging during the process of contact

(see Figs. 14 and 15). Compare with HA impedance controller, for different contact objects, the contact force controlled by the conventional impedance controller appears strong jitter during the process of contact, and its value sometimes is much higher than the desired force (see Figs 15(a) and 16(a)). The phenomenon shows that the change of the external environment (such as position and parameters) effects the force limited function and tracking characteristic of the conventional impedance controller. As Fig. 15(c) described, the maximum tracking error can reach to 4N. Therefore, HA impedance controller has better force tracking characteristic, environmental adaptability and robustness than the conventional impedance controller.

VI. CONCLUSION

Because the external environment is nonlinear, time-variable and unpredictable, the conventional impedance controller with linear dynamic model and constant parameters always has a poor tracking characteristic and adaptability. This problem affects its control performance, which maybe inflict damage on humans, robots or operation objects. In this paper, Hammerstein adaptive (HA) impedance control system made of an outer HA impedance controller and an inner position controller, has been proposed for solving the problem. The outer HA impedance controller is based on the Hammerstein impedance model which is a nonlinear model. In this model, the conventional impedance linear model and a third order nonlinear polynomial are introduced so that the nonlinear of the environment can be described. In order to make the model have a good adaptability, an adaptive law is also designed by using a Lyapunov function. In addition, we select the parameters self-adjust model-free adaptive controller (PSA-MFAC) as the inner position controller. So, the whole HA impedance control system doesn't need the knowledge of the robot dynamics.

Moreover, some simulations and experiments are conducted for verifying the force control performance of proposed control system. The results show that HA impedance control system not only has a better force tracking characteristic than the conventional impedance control system with the same position controller, but also has a good environmental adaptability and robustness for the nonlinear, time-variable and unpredictable environment.

ACKNOWLEDGMENT

The authors thank sincerely the reviewers and editors for their very pertinent remarks that helped this article become clearer and more precise.

REFERENCES

[1] N. Hogan, "Impedance control: An approach to manipulation," *J. Dyn. Syst. Meas. Control*, vol. 107, no. 1, pp. 1–24, 1985.

[2] M. H. Raibert and J. J. Craig, "Hybrid position/force control of manipulators," *J. Dyn. Syst., Meas., Control*, vol. 103, no. 2, pp. 126–133, 1981.

[3] K. Yoshida, H. Nakanishi, H. Ueno, N. Inaba, T. Nishimaki, and M. Oda, "Dynamics, control and impedance matching for robotic capture of a non-cooperative satellite," *Adv. Robot.*, vol. 18, no. 2, pp. 175–198, 2004.

[4] S. Arimoto, H.-Y. Han, C. C. Cheah, and S. Kawamura, "Extension of impedance matching to nonlinear dynamics of robotic tasks," *Syst. Control Lett.*, vol. 36, no. 2, pp. 109–119, 1999.

[5] C. C. Cheah and D. Wang, "Learning impedance control for robotic manipulators," *IEEE Trans. Robot. Autom.*, vol. 14, no. 3, pp. 452–465, Jun. 1998.

[6] F. Ficuciello, L. Villani, and B. Siciliano, "Variable impedance control of redundant manipulators for intuitive human–robot physical interaction," *IEEE Trans. Robot.*, vol. 31, no. 4, pp. 850–863, Aug. 2015.

[7] V. Khoshdel, A. Akbarzadeh, and H. Moeenfard, "Variable impedance control for rehabilitation robot using interval type-2 fuzzy logic," *Int J. Robot*, vol. 4, no. 3, pp. 46–54, 2015.

[8] O. Ryuta, K. Hiroaki, and I. Ryota, "Adaptive impedance control of a variable stiffness actuator," *Adv. Robot.*, vol. 29, no. 4, pp. 273–286, 2015.

[9] J. Koivumäki and J. Mattila, "Stability-guaranteed impedance control of hydraulic robotic manipulators," *IEEE/ASME Trans. Mechatronics*, vol. 22, no. 2, pp. 601–612, Apr. 2017.

[10] M. Sharifi, S. Behzadipour, and G. Vossoughi, "Nonlinear model reference adaptive impedance control for human–robot interactions," *Control Eng. Pract.*, vol. 32, no. 11, pp. 9–27, 2014.

[11] A. Toedtheide, T. Lilge, and S. Haddadin, "Antagonistic impedance control for pneumatically actuated robot joints," *IEEE Robot. Auto. Lett.*, vol. 1, no. 1, pp. 161–168, Jan. 2016.

[12] Z. Li, Z. Huang, W. He, and C.-Y. Su, "Adaptive impedance control for an upper limb robotic exoskeleton using biological signals," *IEEE Trans. Ind. Electron.*, vol. 64, no. 2, pp. 1664–1674, Feb. 2017.

[13] P. K. Jamwal, S. Hussain, M. H. Ghayesh, and S. V. Rogozina, "Impedance control of an intrinsically compliant parallel ankle rehabilitation robot," *IEEE Trans. Ind. Electron.*, vol. 63, no. 6, pp. 3638–3647, Jun. 2016.

[14] D. Zhang, X. Zhao, and J. Han, "Active model-based control for pneumatic artificial muscle," *IEEE Trans. Ind. Electron*, vol. 64, no. 2, pp. 1686–1695, Feb. 2017.

[15] R. Colbaugh, H. Seraji, and K. Glass, "Direct adaptive impedance control of robot manipulators," *J. Robot. Syst.*, vol. 10, no. 2, pp. 217–248, 1993.

[16] B. Heinrichs, N. Sepehri, and A. B. Thornton-Trump, "Position-based impedance control of an industrial hydraulic manipulator," *IEEE Control Syst. Mag.*, vol. 17, no. 1, pp. 46–52, Feb. 1997.

[17] M. Pelletier and M. Doyon, "On the implementation and performance of impedance control on position controlled robots," in *Proc. IEEE Int. Conf. Robot. Autom.*, May 1994, pp. 1228–1233.

[18] W. He, Y. Dong, and C. Su, "Adaptive neural impedance control of a robotic manipulator with input saturation," *IEEE Trans. Syst., Man, Cybern. B, Cybern.*, vol. 40, no. 3, pp. 334–344, Mar. 2016.

[19] T. Kim, H. S. Kim, and J. Kim, "Position-based impedance control for force tracking of a wall-cleaning unit," *Int. J. Precis. Eng. Manuf.*, vol. 17, no. 3, pp. 323–329, 2016.

[20] I. W. Hunter and M. J. Korenberg, "The identification of nonlinear biological systems: Wiener and Hammerstein cascade models," *Biol. Cybern.*, vol. 55, no. 3, pp. 135–144, 1986.

[21] Y. Xi and F. Pang, "Nonlinear adaptive predictive functional control using Hammerstein models," *Syst. Eng. Electron.*, vol. 30, no. 11, pp. 2237–2240, 2008.

[22] M. Yamakita *et al.*, "Development of an artificial muscle linear actuator using ionic polymer–metal composites," *Adv. Robot.*, vol. 18, no. 4, pp. 383–399, 2004.

[23] Y. Guo, J. Mao, and K. Zhou, "Rate-dependent modeling and H_∞ robust control of GMA based on Hammerstein model with Preisach operator," *IEEE Trans. Control Syst. Technol.*, vol. 23, no. 6, pp. 2432–2439, Nov. 2015.

[24] F. Khani and M. Haeri, "Robust model predictive control of nonlinear processes represented by Wiener or Hammerstein models," *Chem. Eng. Sci.*, vol. 129, pp. 223–231, Jun. 2015.

[25] H. Seraji and R. Colbaugh, "Force tracking in impedance control," *Int. J. Robot. Res.*, vol. 16, no. 1, pp. 97–117, Feb. 1997.

[26] E. Eskinat, S. H. Johnson, and W. L. Luyben, "Use of Hammerstein models in identification of nonlinear systems," *AIChE J.*, vol. 37, no. 2, pp. 255–268, 1991.

[27] D. T. Westwick and R. E. Kearney, "Separable least squares identification of nonlinear Hammerstein models: Application to stretch reflex dynamics," *Ann. Biomed. Eng.*, vol. 29, no. 8, pp. 707–718, 2001.

[28] S. Bashash and N. Jalili, "A polynomial-based linear mapping strategy for feedforward compensation of hysteresis in piezoelectric actuators," *J. Dyn. Syst., Meas. Control*, vol. 130, no. 3, pp. 031008-1–031008-10, 2008.

[29] H. Ni and L.-X. Tian, "The integrability and existence of periodic solutions on a first-order nonlinear differential equation with a polynomial nonlinear term," *Math. Problems Eng.*, vol. 2012, Oct. 2012, Art. no. 703474.
[30] Y. Zhu and Z. Hou, "Data-driven MFAC for a class of discrete-time nonlinear systems with RBFNN," *IEEE Trans. Neural Netw. Learn. Syst.*, vol. 25, no. 5, pp. 1013–1020, May 2014.

HUI YANG (S'15) was born in Jinzhou, China, in 1987. He received the B.S. degree and the M.S. degree in machinery design and manufacture from Liaoning Shihua University, Fushun, China, in 2010 and 2013, respectively. He is currently pursuing the Ph.D. degree with Northeastern University, Shenyang, China. His research interests include modeling and control of PAM and compliance control of the bionic manipulator actuated by artificial muscles. He is a Student Member the International Society of Bionic Engineering.

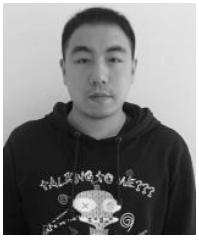

XIFENG GAO was born in Shenyang, China, in 1990. He received the B.S. degree in mechanical design, manufacturing and automation and the M.S. degree in mechanical engineering from the Hebei University of Technology, Tianjin, China, in 2013 and 2016, respectively. He is currently pursuing the Ph.D. degree with Northeastern University, Shenyang. His research interests include modeling and control of artificial muscles, especially in PAM, soft robotics, and robot trajectory planning and system control.

YANG CHEN (S'15) was born in Qitaihe, China, in 1988. He received the B.S. degree in mechanical engineering and automation from the China University of Mining and Technology, Xuzhou, China, in 2012, and the M.S. degree in mechatronic engineering from Northeastern University, Shenyang, China, in 2014, where he is currently pursuing the Ph.D. degree. His research interests include driving, modeling and control of artificial muscles especially in IPMC and SMA, and soft robotic hand. He is a Student Member the International Society of Bionic Engineering.

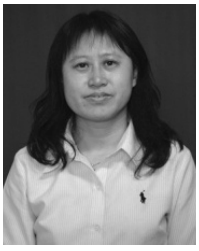

LINA HAO was born in Zhuanghe, China, in 1968. She received the B.S. degree in machinery design and manufacture from Shenyang Ligong University, Shenyang, China, in 1989, and the M.S. degree in solid mechanics and the Ph.D. degree in control theory and control engineering from Northeastern University, Shenyang, in 1994 and 2001, respectively. She is currently a Professor with the Department of Mechanical Engineering and Automation, Northeastern University. Her research interests include robot system and intelligent control, intelligent structure and precision motion control system, pattern recognition, and condition monitoring. She is a member of the International Society of Bionic Engineering and the Chinese Association of Automation System Simulation Discipline and Robot Discipline Committee. She is selected as a hundred-level member in the Pacesetter Project of Liaoning, China.